Received 27 July 2023; revised 6 November 2023; accepted 2 December 2023. Date of publication 6 December 2023; date of current version 29 December 2023.

Digital Object Identifier 10.1109/OJCOMS.2023.3339790

Performance of RSMA-Based UOWC Systems Over Oceanic Turbulence Channel With Pointing Errors

ZIYAUR RAHMAN (Student Member, IEEE), IMENE ROMDHANE (Student Member, IEEE), AND GEORGES KADDOUM (Senior Member, IEEE)

Department of Electrical Engineering, École de Technologie Supérieure, Montreal, QC H3C 1K3, Canada

CORRESPONDING AUTHOR: I. ROMDHANE (e-mail: imene.romdhane.1@ens.etsmtl.ca)

This work was supported in part by the ULTRA TCS Research Chair on Intelligent Tactical Wireless Networks for Challenging Environments and in part by the National Natural Sciences and Engineering Research Council of Canada (NSERC) under Grant CRDPJ 538896-19.

ABSTRACT Underwater optical wireless communication (UOWC) systems face significant challenges due to oceanic turbulence and pointing errors (PE), which can degrade system performance. Moreover, interference is another challenge in UOWC, considering the consistent increase in underwater optical devices. In this study, the performance of rate splitting multiple access (RSMA)-based UOWC systems is investigated over an exponential-generalized gamma (EGG)-distributed oceanic turbulence channel with generalized PE. The RSMA scheme is employed to facilitate communication between a source and multiple users in the UOWC system while accounting for the combined effects of oceanic turbulence and generalized PE. The statistical characterization of the UOWC system is analyzed, including the probability density function (PDF) of the signal-to-noise ratio (SNR), outage probability, throughput, and sum ergodic capacity. Additionally, closed-form expressions for the outage probability and throughput are derived, and asymptotic expressions for the outage probability in the high SNR regime are provided. Moreover, the diversity order of the system is evaluated, and the impact of different parameters on the system performance is discussed. Our results demonstrate the effectiveness of the RSMA-based UOWC system in mitigating the adverse effects of oceanic turbulence and PE while achieving improved performance in terms of capacity and outage probability. The findings of this study provide valuable insights for the design and optimization of UOWC systems in challenging underwater environments.

INDEX TERMS EGG model, non-zero boresight pointing errors, oceanic turbulence, outage probability, performance analysis, sum ergodic capacity.

I. INTRODUCTION

UNDERWATER wireless communications are of paramount importance in the field of communications. The ability to establish reliable and efficient underwater communication links opens up a wide range of applications and opportunities for various industries and scientific research. Radio frequency (RF) signals can penetrate the water surface to a certain depth, allowing for limited underwater communication. Acoustic waves, on the other hand, can travel long distances through water, making them a practical choice for underwater communication over extended ranges. However, RF communications are energy intensive [1], [2], and acoustic communications are characterized by low speed and limited bandwidth [3], [4]. Consequently, underwater optical wireless communication (UOWC) has been recently proposed as a promising alternative for marine communications. UOWCs are mainly based on light exchange between different underwater communication sensors. This technology is characterized by high data rates in the order of Gbps, low-cost implementation, low power consumption, and low latency [5]. Nevertheless, UOWCs are highly affected by underwater turbulence and pointing errors (PE), where the transmitted beam is not perfectly facing the receiver. This significantly degrades the link quality and connectivity of such communication systems. Moreover, the upsurge of UOWC applications has led to a remarkable increase in optical devices underwater. This has resulted in denser underwater optical networks, emphasizing the impact of interference on UOWC systems. The interference between different optical links can further deteriorate the

© 2023 The Authors. This work is licensed under a Creative Commons Attribution 4.0 License. For more information, see https://creativecommons.org/licenses/by/4.0/

communication quality of the transmitted signals. Hence, studying the performance of such links becomes crucial.

Several statistical models were proposed in the literature to model underwater turbulence, namely the lognormal, log-logistic, gamma, exponential Weibull (EW), and generalized gamma (GG) distributions [6], [7]. The exponential-generalized gamma (EGG) is another distribution that was recently introduced as a perfect model for air bubbles and temperature-induced oceanic turbulence under different channel conditions [8]. Considering its ability to various oceanic turbulence levels in a unified manner, we select the EGG distribution to model the oceanic turbulence in our system.

Another challenge faced by multi-user UOWC systems is the interference between the different optical links. The increase of devices deployed underwater led to denser networks, and consequently stronger interference effects. In this regard, different multiple access schemes have been proposed to mitigate the interference effect on the system's performance. Space division multiple access (SDMA) and non-orthogonal multiple access (NOMA) are two adopted multi-access schemes in the literature, to name a few. In SDMA, users are separated in the spatial domain using a linear precoding technique, and the residual interference between users is considered as noise. As for NOMA, users are superposed in the power domain using linearly precoded superposition coding with successive interference cancellation (SIC)-based decoding. This technique is based on user grouping and ordering and enforces some users to fully decode and omit the interference generated by other users. These multi-access schemes indeed enhance the performance of multi-user systems by enabling multiple users to simultaneously transmit over the same resource block. However, they are extreme techniques as they fully treat interference as noise (i.e., SDMA) or fully decode the interference (i.e., NOMA). This extreme behavior degrades the performance of SDMA with the increase in the number of users as more transmit antennas are needed to effectively manage the multi-user interference, and remarkably increases the complexity of NOMA with the increase in the number of users. Hence, the performance of these multiple access schemes is limited in dense networks [9]. As an alternative, the rate splitting multiple access (RSMA) scheme was proposed to overcome the aforementioned complexity issue. This technique was shown to be promising in terms of robustness, low complexity, and high spectral efficiency. RSMA can be considered as a combination between of NOMA and SDMA. Relying on linearly precoded rate splitting (RS) at the transmitter and SIC at the receivers, the interference is partially decoded and partially treated as noise. It is, therefore, a softer interference management scheme compared to NOMA and SDMA.

A. RELATED WORK

Several papers have considered the EGG distribution for modeling underwater turbulence in the literature. In [10], a NOMA-based reflecting intelligent surface (RIS)-assisted hybrid RF-UOWC system is assessed considering the EGG turbulence model for the optical link without PE. The performance of multi-hop UOWC systems is analyzed in [11] using both amplify-and-forward (AF) and decode-and-forward (DF) relaying schemes, considering the EGG turbulence model without PE. Authors in [12] study a vertical multi-layer underwater wireless optical communication (UWOC) system using EGG distribution without PE. In [13], [14], hybrid terrestrial-underwater wireless optical communications are considered assuming the EGG underwater turbulence with zero boresight PE model.

In [15], the selection combining technique is used for a hybrid RF-UWOC system, where the RF link is a backup for the optical link, which is modeled as an EGG turbulence link without PE. AF and DF relaying schemes are used in [16], [17], [18], [19] for joint RF-UOWC systems considering EGG underwater turbulence for the optical link without PE. In [20], the AF relaying scheme is proposed for hybrid free space optical (FSO)-UWOC systems using the EGG turbulence with zero-boresight PE model for the UOWC link.

Recently, RSMA has emerged as a promising solution for enhancing the spectrum efficiency of wireless systems. It has been considered by numerous researchers in terrestrial RF communications. Authors in [21], [22], [23] investigate the RSMA for the downlink transmission in unmanned aerial vehicle (UAV)-based systems to increase the data rate, throughput, and ergodic capacity. The RSMA scheme is analyzed in [24] for RIS-assisted UAV-based multi-user communication networks in the presence of co-channel interference. In [25], RSMA is proposed for uplink between ultra-reliable low-latency communication (URLLC) users and the base station (BS) to improve the communication's sum rate and reliability. Researchers in [26] study the energy efficiency of RSMA-based and RIS-assisted wireless communication systems. The RSMA technique is also employed in satellite communications to increase the sum rate and optimize the power budget in [27].

In addition to RF communications, many researchers use RSMA in visible light communications (VLCs). In [28], [29], [30], the RSMA technique is used in VLC networks to improve the system's sum rate compared to NOMA or SDMA. It is also demonstrated in [31] that RSMA-based VLC broadcast systems achieve better energy efficiency than NOMA-based and SDMA-based VLC systems. Researchers in [32] introduce a single-layer RSMA-based VLC system that maximizes the spectral efficiency under the constraint of the non-linear effect of a light-emitting diode (LED), compared to NOMA-based VLC systems. Considering the benefits of RSMA on the system's performance, this technique was recently introduced in UOWC systems as well. In [33], the ergodic rate of an RSMA-based UOWC system is assessed, where log-normal weak oceanic turbulence is considered without PE. However, to the best of the authors' knowledge, there are no existing results for the performance of RSMA-based UOWC

TABLE 1. Summary of related literature.

Reference	Turbulence	PE	System Model	Technique used
[10]	EGG	✗	RF-UOWC	NOMA
[11]	EGG	✗	Multi-Hop UWOC	AF & DF
[12]	EGG	✗	UWOC	Multi-layers
[13], [14]	EGG	Zero boresight	TWOC-UWOC	Single-layer, Multi-layers
[15]	EGG	✗	hybrid RF/UWOC	Selection combine
[16]–[19]	EGG	✗	RF-UWOC	AF & DF
[20]	EGG	Zero boresight	FSO-UWOC	AF
[21]–[26]	✗	✗	RF	RSMA
[27]	✗	✗	Satellite communications	RSMA
[28]–[32]	✗	✗	VLC	RSMA
[33]	Log-Normal	✗	UWOC	RSMA
[Proposed]	EGG	generalized	UWOC	RSMA

TWOC: Terrestrial wireless optical communication

systems over EGG turbulence with a generalized PE model. In Table 1, we present a comprehensive state-of-the-art summary. This table provides an overview of the key considerations, system models, and techniques employed in various studies conducted in the literature. It serves as a valuable reference for understanding the advancements and current state of research in UOWC systems and RSMA, highlighting the different aspects researchers have focused on and the approaches they have taken to address the challenges faced.

B. NOVELTY AND CONTRIBUTIONS

In this paper, we use the RSMA for communication between a source and multiple users over an underwater wireless link. We consider the combined impact of oceanic turbulence and generalized PE in our analysis. The novelty and contributions of this work can be summarized as follows:

- We assess the performance of RSMA-based multi-user downlink UOWC over EGG oceanic turbulence with generalized PE.
- We derive a novel analytical expression for the probability density function (PDF) of the signal-to-noise ratio (SNR) over EGG-distributed oceanic turbulence and generalized PE.
- We derive the exact expression of the outage probability and throughput of RSMA-based multi-user UOWC considering the joint effect of oceanic turbulence and PE. The asymptotic expressions of these two metrics are also derived in this work.
- We develop an analytical approximation for the ergodic capacity along with its corresponding asymptotic expression.
- The diversity order of the studied system is derived from the asymptotic expressions of the outage probability, throughput, and ergodic capacity.
- The performance of the proposed system in terms of outage probability, throughput, and ergodic capacity metrics is assessed using simulations considering different oceanic turbulence and PE values.
- The effect of the number of users and the resource distribution among the broadcast and private links on the performance of the proposed system is assessed through simulations.

C. NOTATIONS AND ORGANIZATION

Notations: $(\cdot)_i$ denotes parameters for the i-th user, N denotes the total number of users. We represent the zero-order modified Bessel function of the first kind by $I_0(\cdot)$ [34, eq. (8).431.1], Gamma function by $\Gamma(a) = \int_0^\infty t^{a-1}e^{-t}dt$, and Meijer G-function by $G^{m,n}_{p,q}\left[z\middle|\begin{matrix}(a_k)_{k=1:p}\\(b_k)_{k=1:q}\end{matrix}\right]$.

Organization: The remainder of this paper is structured as follows. Section II provides a detailed explanation of the channel model, including EGG distributed oceanic turbulence and generalized PE, for RSMA-based multi-user UOWC systems. In Sections III and IV, we present the statistical characterization and performance evaluation of UOWC systems, focusing on the PDF of the SNR, outage probability, throughput, and sum ergodic capacity. Section V showcases simulation results and discussions. Finally, in Section VI, we conclude this paper.

II. SYSTEM MODEL

We consider a downlink multi-user UOWC system (as shown in Fig. 1) that uses RSMA signaling to transmit information data to N users $(D_1, D2, \ldots, D_N)$, simultaneously. The quality of the transmitted signal is degraded by various multiplicative channel effects, including path loss, oceanic turbulence, and PE. Therefore, the channel coefficient between the source and D_i is given as:

$$h_i = h_{l_i} h_{t_i} h_{p_i}, \tag{1}$$

where $h_{l_i} = e^{-\alpha d}$ is the oceanic path loss coefficient, d is the link distance in meters, and α is the extinction attenuation coefficient. Moreover, h_{t_i} is the EGG-distributed oceanic

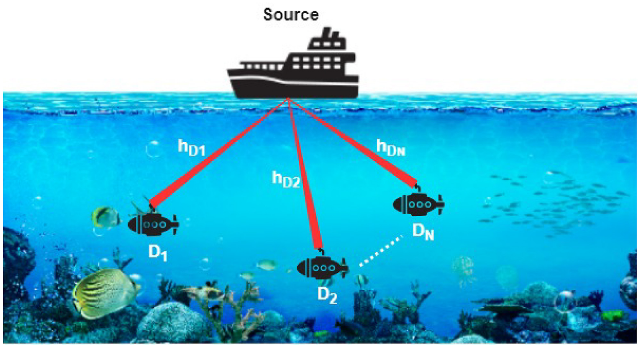

FIGURE 1. RSMA-based UOWC system, D: Destination, h_D: Channel gain.

turbulence, and h_{p_i} is the Rician-distributed PE with non-zero boresight and random jitter. The PDF of h_{t_i} is given as [8]:

$$f_{h_{t_i}}(x) = \frac{\omega_i}{x} G_{0,1}^{1,0}\left(\begin{matrix} - \\ 1 \end{matrix} \middle| \frac{x}{\lambda_i} \right) + \frac{c_i(1-\omega_i)}{\Gamma(a_i)x} G_{0,1}^{1,0}\left(\begin{matrix} - \\ a_i \end{matrix} \middle| \left(\frac{x}{b_i}\right)^{c_i} \right), \tag{2}$$

where λ_i, a_i, b_i, c_i, and ω_i represent the parameters of the EGG distribution, satisfying the condition $0 < \omega_i < 1$.

The PDF of h_{p_i} is given as [35], [36]:

$$f_{h_{p_i}}(x) = \frac{\rho_i^2 \exp\left(\frac{-s_i^2}{2\sigma_i^2}\right)}{A_i^{\rho_i^2}} x^{\rho_i^2-1} I_0\left(\frac{s_i}{\sigma_i^2} \sqrt{\frac{w_{z_{\mathrm{eq_i}}}^2 \ln \frac{A_i}{x}}{2}} \right), \tag{3}$$

where $0 \leq x \leq A_i$. The parameter $w_{z_{\mathrm{eq_i}}}^2$ is defined as $w_{z_{\mathrm{eq_i}}}^2 = \frac{w_{z_i}^2 \sqrt{A_i \pi}}{2v_i \exp(-v_i^2)}$, with $A_i = [\mathrm{erf}(v_i)]^2$, where $v_i = \sqrt{\frac{r_i^2 \pi}{2w_{z_i}^2}}$ represents the ratio of aperture radius r_i to beamwidth w_{z_i}. Furthermore, ρ_i is defined as $\rho_i = \frac{w_{z_{\mathrm{eq_i}}}}{2\sigma_i}$, where σ_i denotes the standard deviation of the jitter and $w_{z_{\mathrm{eq_i}}}$ represents the equivalent beamwidth. In this context, $s_i = \sqrt{\mu_{x_i}^2 + \mu_{y_i}^2} \neq 0$ is used to model the non-zero boresight, where $\mu_{x_i} \neq 0$ and $\mu_{y_i} \neq 0$ indicate the horizontal and vertical displacements between the center of the beam and the center of the detector, respectively. It is important to note that the presented in (3) is a generalized distribution, which includes the special case of zero boresight for $s_i = 0$ [37].

In the RSMA scheme, each user's message is divided into two parts: common message and private message. The common messages from all the users are combined and encoded into a unified common message (s_c) using a common codebook accessible to all the users. Additionally, the private message of user D_i is encoded as private message s_i. The unified common message (s_c) represents the portion of the message shared among all users and is decoded by each user. On the other hand, the private message s_i is specifically intended for user D_i and is only decoded by D_i. Consequently, the superimposed symbol transmitted by the source can be expressed as follows:

$$s = \sqrt{a_c P_t} s_c + \sum_{i=1}^{N} \sqrt{a_{p_i} P_t} s_i, \tag{4}$$

where P_t denotes the optical transmit power at the source. The power coefficients allocated to the common and private messages are denoted as a_c and a_{p_i}, respectively, satisfying the constraint $a_c + \sum_{i=1}^{N} a_{p_i} = 1$. The signal received at the i-th user can be expressed as:

$$y_i = h_i s + n_i = \underbrace{\sqrt{a_c P_t} h_i s_c}_{\text{Common message}} + \underbrace{\sqrt{a_{p_i} P_t} h_i s_i}_{\text{Private message}} + \underbrace{\sum_{j=1, i\neq j}^{N} \sqrt{a_{p_j} P_t} h_i s_j}_{\text{interference}} + \underbrace{n_i}_{\text{AWGN}}, \tag{5}$$

where n_i represents the additive white Gaussian noise (AWGN) with zero mean and variance $\sigma_{n_i}^2$. Based on (5), it is evident that in addition to the intended common and private messages, each user also receives private messages from other users, resulting in interference during the decoding process. As a result, each user employs a two-step decoding approach to extract the desired information from the received signal. In the first step, the common message is decoded, considering all other messages as interference. Using the non-coherent intensity modulation/direct detection (IM/DD) scheme, the corresponding signal-to-interference plus noise ratio (SINR) for decoding the common message at the i-th user can be expressed as follows:

$$\gamma_{c,i} = \frac{a_c \gamma_i}{1 + \gamma_i (1 - a_c)}, \tag{6}$$

where $\gamma_i = \frac{P_t^2 h_i^2}{\sigma_{n_i}^2} = \gamma_0 |h_{t_i} h_{p_i}|^2$ with $\gamma_0 = \frac{P_t^2 h_{l_i}^2}{\sigma_{n_i}^2}$ being the instantaneous SNR of the on-off keying (OOK) signaling scheme. Upon successful decoding of the common message, each user proceeds to the second step, where they decode their desired private messages. This is achieved by subtracting the decoded common message from the received signal while considering the private messages of all other users as interference. The SINR for decoding the private message at the i-th user can be expressed as follows:

$$\gamma_{p,i} = \frac{a_i \gamma_i}{1 + \gamma_i \sum_{j=1, i\neq j}^{N} a_{p_j}}. \tag{7}$$

III. STATISTICAL CHARACTERIZATION

In this section, we derive a novel closed-form expression for the PDF of the SNR over combined EGG-distributed oceanic turbulence and generalized PE.

Theorem 1: The SNR PDF over EGG distributed oceanic turbulence and generalized PE for UOWC is given as:

$$f_{\gamma_i}(\gamma) = \frac{\omega_i \rho_i^2 \exp\left(\frac{-s_i^2}{2\sigma_i^2}\right)}{2\gamma} \sum_{j'=0}^{\infty} \frac{1}{j'!} \left(\frac{s_i^2 w_{z_{\mathrm{eq_i}}}^2}{8\sigma_i^4} \right)^{j'} \times G_{1+j',2+j'}^{2+j',0}\left(\begin{matrix} \{\rho_i^2+1\}^{j'+1} \\ 1, \{\rho_i^2\}^{j'+1} \end{matrix} \middle| \frac{1}{\lambda_i A_i} \sqrt{\frac{\gamma}{\gamma_0}} \right)$$

$$+\frac{(1-\omega_i)\rho_i^2\exp\left(\frac{-s_i^2}{2\sigma_i^2}\right)}{2\gamma\Gamma(a_i)}\sum_{j'=0}^{\infty}\frac{1}{j'!}\left(\frac{s_i^2 w_{z_{\mathrm{eq_i}}}^2}{8\sigma_i^4}\right)^{j'}$$
$$\times G_{1+j',2+j'}^{2+j',0}\left(\begin{matrix}\{\frac{\rho_i^2}{c_i}+1\}^{j'+1}\\ a_i,\{\frac{\rho_i^2}{c_i}\}^{j'+1}\end{matrix}\middle|\left(\frac{1}{b_iA_i}\sqrt{\frac{\gamma}{\gamma_0}}\right)^{c_i}\right). \quad (8)$$

Proof: Since it is intractable to find the closed form expression of combined SNR PDF with the modified Bessel function, we employ the series expansion of the modified Bessel function $I_0(x)=\sum_{j'=0}^{\infty}\frac{(\frac{x}{2})^{2j'}}{(j'!)^2}$ in (3) to get:

$$f_{h_{p_i}}(x)=\frac{\rho_i^2\exp\left(\frac{-s_i^2}{2\sigma_i^2}\right)}{A_i^{\rho_i^2}}\sum_{j'=0}^{\infty}\frac{1}{(j'!)^2}\left(\frac{s_i^2 w_{z_{\mathrm{eq_i}}}^2}{8\sigma_i^4}\right)^{j'}x^{\rho_i^2-1}\left(\ln\frac{A_i}{x}\right)^{j'}. \quad (9)$$

It is important to note that the converging series expansion presented in (9) enables us to analyze the system performance effectively. The authors in [38] have presented a plot that demonstrates the convergence of the series expansion employed in (9). The plot shows that the series converges rapidly, where approximately 20 terms is sufficient for accurate approximation.

Applying the theory of product distribution, the PDF of $h_{tp_i}=h_{p_i}h_{t_i}$ can be expressed as:

$$f_{h_{tp_i}}(x)=\int_0^{A_i}\frac{1}{|h_{p_i}|}f_{h_{t_i}}(x/h_{p_i})f_{h_{p_i}}(h_{p_i})dh_{p_i}. \quad (10)$$

Substituting (9) and (2) in (10), and taking the integral definition of Meijer's G-function, we get:

$$f_{h_{tp_i}}(x)=\frac{\omega_i\rho_i^2\exp\left(\frac{-s_i^2}{2\sigma_i^2}\right)}{xA_i^{\rho_i^2}}\sum_{j'=0}^{\infty}\frac{1}{(j'!)^2}\left(\frac{s_i^2 w_{z_{\mathrm{eq_i}}}^2}{8\sigma_i^4}\right)^{j'}$$
$$\left(\frac{1}{2\pi\jmath}\int_{\mathcal{L}}\Gamma(1-u)\left(\frac{x}{\lambda_i}\right)^{u}du\right)I_1+\frac{c_i(1-\omega_i)\rho_i^2\exp\left(\frac{-s_i^2}{2\sigma_i^2}\right)}{\Gamma(a_i)xA_i^{\rho_i^2}}$$
$$\sum_{j'=0}^{\infty}\frac{1}{(j'!)^2}\left(\frac{s_i^2 w_{z_{\mathrm{eq_i}}}^2}{8\sigma_i^4}\right)^{j'}\left(\frac{1}{2\pi\jmath}\int_{\mathcal{L}}\Gamma(a_1-u)\left(\frac{x}{b_i}\right)^{c_iu}du\right)I_2, \quad (11)$$

where $I_1=\int_0^{A_i}h_{p_i}^{\rho_i^2-u-1}(\ln\frac{A_i}{h_{p_i}})^{j'}dh_{p_i}$ and $I_2=\int_0^{A_i}h_{p_i}^{\rho_i^2-c_iu-1}(\ln\frac{A_i}{h_{p_i}})^{j'}dh_{p_i}$.

After substituting $\log\frac{A_i}{h_{p_i}}=t$ to solve the inner integrals, I_1 and I_2, we obtain:

$$\begin{aligned}I_1&=A_i^{\rho_i^2-u}\int_0^{\infty}e^{-(\rho_i^2-u)t}t^{j'}dt\\&=A_i^{\rho_i^2-u}\frac{\Gamma(1+j')}{(\rho_i^2-u)^{1+j'}}\\&=A_i^{\rho_i^2-u}\frac{\Gamma(1+j')[\Gamma(\rho_i^2-u)]^{1+j'}}{[\Gamma(1+\rho_i^2-u)]^{1+j'}},\end{aligned} \quad (12)$$

and

$$\begin{aligned}I_2&=A_i^{\rho_i^2-c_iu}\int_0^{\infty}e^{-(\rho_i^2-c_iu)t}t^{j'}dt\\&=A_i^{\rho_i^2-c_iu}\frac{\Gamma(1+j')}{(\rho_i^2-c_iu)^{1+j'}}\\&=A_i^{\rho_i^2-c_iu}\frac{\Gamma(1+j')[\Gamma(\rho_i^2-c_iu)]^{1+j'}}{[\Gamma(1+\rho_i^2-c_iu)]^{1+j'}}.\end{aligned} \quad (13)$$

Now, we substitute (12) and (13) in (11) and apply Meijer's G-function. Using the transformation $\gamma_i=\gamma_0|h_{tp}|^2$, we get the SNR PDF for UOWC in (8). ■

IV. PERFORMANCE ANALYSIS

In this section, we derive closed-form expressions for the outage probability and throughput, as well as analytical expressions for the ergodic sum rate of RSMA-based multiuser UOWC. The analysis takes into account oceanic turbulence following the EGG distribution and generalized PE.

A. OUTAGE PROBABILITY AND THROUGHPUT

In RSMA, if the SINRs for decoding the common and private messages fall below certain threshold values, $\gamma_{\mathrm{th}}^{c,i}$ and $\gamma_{\mathrm{th}}^{p,i}$ respectively, an outage occurs in the link between the UAV-BS and i-th user. Specifically, $\gamma_{\mathrm{th}}^{c,i}$ is set' to $2^{2R_{c,i}-1}$, representing the target rate for decoding the common message, and $\gamma_{\mathrm{th}}^{p,i}$ is set to $2^{2R_{p,i}-1}$, representing the target rate for decoding the private message.

Theorem 2: The outage probability of the RSMA-based multi-user UOWC link between the source and the i-th user is given in (14), at the bottom of the next page, where $\hat{\gamma}_{\mathrm{th}}^{c,i}=\frac{\gamma_{\mathrm{th}}^{c,i}}{\gamma_0(a_c-(1-a_c)\gamma_{\mathrm{th}}^{c,i})}$, $\hat{\gamma}_{\mathrm{th}}^{p,i}=\frac{\gamma_{\mathrm{th}}^{p,i}}{\gamma_0(a_{p_i}-(1-a_c-a_{p_i})\gamma_{\mathrm{th}}^{p,i})}$, $a_c>\frac{\gamma_{\mathrm{th}}^{c,i}}{(1+\gamma_{\mathrm{th}}^{c,i})}$, and, $a_{p_i}>\frac{(1-a_c)\gamma_{\mathrm{th}}^{p,i}}{(1+\gamma_{\mathrm{th}}^{p,i})}$.

Proof: The outage probability of the i-th user can be expressed as follows:

$$P_{\mathrm{out_i}}=1-\Pr\left(\gamma_{c,i}>\gamma_{\mathrm{th}}^{c,i},\gamma_{p,i}>\gamma_{\mathrm{th}}^{p,i}\right). \quad (15)$$

Using the SINRs of the common and private messages from (6) and (7) in (15), we get:

$$P_{\mathrm{out_i}}=1-\Pr\left(\frac{\mathrm{a_c}\gamma_\mathrm{i}}{1+\gamma_\mathrm{i}(1-\mathrm{a_c})}>\gamma_{\mathrm{th}}^{\mathrm{c,i}},\frac{\mathrm{a_{p_i}}\gamma_\mathrm{i}}{1+\gamma_\mathrm{i}\mathrm{B}}>\gamma_{\mathrm{th}}^{\mathrm{p,i}}\right), \quad (16)$$

where $B=\sum_{j=1,i\neq j}^{N}a_{p_j}$. After some algebraic manipulations (16) can be written as:

$$P_{\mathrm{out_i}}=1-\Pr\left(\gamma_i>\hat{\gamma}_{I\mathrm{th}}^{c,i},\gamma_i>\hat{\gamma}_{\mathrm{th}}^{p,i}\right)=\Pr\left(\gamma_i\leq\hat{\gamma}_{\mathrm{th}}\right), \quad (17)$$

where $\hat{\gamma}_{\mathrm{th}}=\max(\hat{\gamma}_{\mathrm{th}}^{c,i},\hat{\gamma}_{\mathrm{th}}^{p,i})$. Using (8) in the above equation, we get:

$$P_{\mathrm{out_i}}=\int_0^{\hat{\gamma}_{\mathrm{th}}}\frac{\omega_i\rho_i^2\exp\left(\frac{-s_i^2}{2\sigma_i^2}\right)}{2\gamma}\sum_{j'=0}^{\infty}\frac{1}{j'!}\left(\frac{s_i^2 w_{z_{\mathrm{eq_i}}}^2}{8\sigma_i^4}\right)^{j'}$$

$$\times G^{2+j',0}_{1+j',2+j'}\left(\begin{matrix}\{\rho_i^2+1\}^{j'+1}\\ 1,\{\rho_i^2\}^{j'+1}\end{matrix}\middle|\frac{1}{\lambda_i A_i}\sqrt{\frac{\gamma}{\gamma_0}}\right)+\frac{(1-\omega_i)\rho_i^2\exp\left(\frac{-s_i^2}{2\sigma_i^2}\right)}{2\gamma\Gamma(a_i)c_i}\sum_{j'=0}^{\infty}\frac{1}{j'!}\left(\frac{s_i^2w_{z_{\mathrm{eq_i}}}^2}{8\sigma_i^4}\right)^{j'}\times G^{2+j',0}_{1+j',2+j'}\left(\begin{matrix}\{\frac{\rho_i^2}{c_i}+1\}^{j'+1}\\ a_i,\{\frac{\rho_i^2}{c_i}\}^{j'+1}\end{matrix}\middle|\left(\frac{1}{b_iA_i}\sqrt{\frac{\gamma}{\gamma_0}}\right)^{c_i}\right)d\gamma. \tag{18}$$

Substituting the integral form of the Meijer-G function and using the inner integral $\int_0^{\hat{\gamma}_{\mathrm{th}}}\gamma^{\frac{u}{2}-1}=\hat{\gamma}_{\mathrm{th}}^{\frac{u}{2}}$, we get:

$$P_{\mathrm{out_i}}=\omega_i\rho_i^2\exp\left(\frac{-s_i^2}{2\sigma_i^2}\right)\sum_{j'=0}^{\infty}\frac{1}{j'!}\left(\frac{s_i^2w_{z_{\mathrm{eq_i}}}^2}{8\sigma_i^4}\right)^{j'}\times G^{2+j',1}_{2+j',3+j'}\left(\begin{matrix}1,\{\rho_i^2+1\}^{j'+1}\\ 1,\{\rho_i^2\}^{j'+1},0\end{matrix}\middle|\frac{1}{\lambda_iA_i}\sqrt{\frac{\hat{\gamma}_{\mathrm{th}}}{\gamma_0}}\right)+\frac{(1-\omega_i)\rho_i^2\exp\left(\frac{-s_i^2}{2\sigma_i^2}\right)}{\Gamma(a_i)c_i}\sum_{j'=0}^{\infty}\frac{1}{j'!}\left(\frac{s_i^2w_{z_{\mathrm{eq_i}}}^2}{8\sigma_i^4}\right)^{j'}\times G^{2+j',1}_{2+j',3+j'}\left(\begin{matrix}1,\{\frac{\rho_i^2}{c_i}+1\}^{j'+1}\\ a_i,\{\frac{\rho_i^2}{c_i}\}^{j'+1},0\end{matrix}\middle|\left(\frac{1}{b_iA_i}\sqrt{\frac{\hat{\gamma}_{\mathrm{th}}}{\gamma_0}}\right)^{c_i}\right). \tag{19}$$

Substituting $\hat{\gamma}_{\mathrm{th}}=\max(\hat{\gamma}_{\mathrm{th}}^{c,i},\hat{\gamma}_{\mathrm{th}}^{p,i})$ in (19), we get the closed-form expressions for the outage probability in (14). ■

To find the diversity order of the proposed system, we derive the asymptotic expansion of the outage probability in the following Lemma.

Lemma 1: To derive the asymptotic expression for the outage probability in the high SNR regime $\gamma_0\to\infty$ in (20), at the bottom of the page, we can utilize the series expansion of the Meijer G-function, where $\mathcal{E}_k=\mathcal{E}_l=\{1,\{\rho_i^2+1\}^{j'+1}\}$, $\mathcal{F}_k=\mathcal{F}_l=\{1,\{\rho_i^2\}^{j'+1},0\}$, $\mathcal{G}_k=\mathcal{G}_l=\{1,\{\frac{\rho_i^2}{c_i}+1\}^{j'+1}\}$, and $\mathcal{H}_k=\mathcal{H}_l=\{a_i,\{\frac{\rho_i^2}{c_i}\}^{j'+1},0\}$.

Proof: Taking the asymptotic expansion of the Meijer-G function, [39, eq. (07).34.06.0006.01] at high SNR ($\gamma_0\to\infty$) in (14), we get the asymptotic expansion of the outage probability in (20). ■

Remark 1: Taking the exponent of γ_0 in (20), the diversity order of the system can be expressed as $G_i=\min\{\frac{1}{2},\frac{\rho_i^2}{2},\frac{a_ic_i}{2}\}$. It is crucial to emphasize that the diversity order remains unchanged and unaffected by the boresight parameters.

Remark 2: It is evident from (14) that the successful decoding of both messages is crucial for enhancing the user's outage performance. Furthermore, parameters, such as the transmit power, power coefficients, target rate, etc., have a direct impact on the user's outage performance. Hence, careful selection of these parameters is crucial to achieve the desired performance. By utilizing (14), the throughput at the i-th user, measured in bits per channel use (bpcu), can

$$P_{\mathrm{out_i}}=\begin{cases}\omega_i\rho_i^2\exp\left(\frac{-s_i^2}{2\sigma_i^2}\right)\sum_{j'=0}^{\infty}\frac{1}{j'!}\left(\frac{s_i^2w_{z_{\mathrm{eq_i}}}^2}{8\sigma_i^4}\right)^{j'}G^{2+j',1}_{2+j',3+j'}\left(\begin{matrix}1,\{\rho_i^2+1\}^{j'+1}\\ 1,\{\rho_i^2\}^{j'+1},0\end{matrix}\middle|\frac{1}{\lambda_iA_i}\sqrt{\hat{\gamma}_{\mathrm{th}}^{p,i}}\right)\\ +\frac{(1-\omega_i)\rho_i^2\exp\left(\frac{-s_i^2}{2\sigma_i^2}\right)}{\Gamma(a_i)c_i}\sum_{j'=0}^{\infty}\frac{1}{j'!}\left(\frac{s_i^2w_{z_{\mathrm{eq_i}}}^2}{8\sigma_i^4}\right)^{j'}G^{2+j',1}_{2+j',3+j'}\left(\begin{matrix}1,\{\frac{\rho_i^2}{c_i}+1\}^{j'+1}\\ a_i,\{\frac{\rho_i^2}{c_i}\}^{j'+1},0\end{matrix}\middle|\left(\frac{1}{b_iA_i}\sqrt{\hat{\gamma}_{\mathrm{th}}^{p,i}}\right)^{c_i}\right), & \text{if } \hat{\gamma}_{\mathrm{th}}^{c,i}\le\hat{\gamma}_{\mathrm{th}}^{p,i}\\ \omega_i\rho_i^2\exp\left(\frac{-s_i^2}{2\sigma_i^2}\right)\sum_{j'=0}^{\infty}\frac{1}{j'!}\left(\frac{s_i^2w_{z_{\mathrm{eq_i}}}^2}{8\sigma_i^4}\right)^{j'}G^{2+j',1}_{2+j',3+j'}\left(\begin{matrix}1,\{\rho_i^2+1\}^{j'+1}\\ 1,\{\rho_i^2\}^{j'+1},0\end{matrix}\middle|\frac{1}{\lambda_iA_i}\sqrt{\hat{\gamma}_{\mathrm{th}}^{c,i}}\right)\\ +\frac{(1-\omega_i)\rho_i^2\exp\left(\frac{-s_i^2}{2\sigma_i^2}\right)}{\Gamma(a_i)c_i}\sum_{j'=0}^{\infty}\frac{1}{j'!}\left(\frac{s_i^2w_{z_{\mathrm{eq_i}}}^2}{8\sigma_i^4}\right)^{j'}G^{2+j',1}_{2+j',3+j'}\left(\begin{matrix}1,\{\frac{\rho_i^2}{c_i}+1\}^{j'+1}\\ a_i,\{\frac{\rho_i^2}{c_i}\}^{j'+1},0\end{matrix}\middle|\left(\frac{1}{b_iA_i}\sqrt{\hat{\gamma}_{\mathrm{th}}^{c,i}}\right)^{c_i}\right), & \text{if } \hat{\gamma}_{\mathrm{th}}^{c,i}\ge\hat{\gamma}_{\mathrm{th}}^{p,i}\end{cases} \tag{14}$$

$$P_{\mathrm{out_i}}^{\infty}=\begin{cases}\omega_i\rho_i^2\exp\left(\frac{-s_i^2}{2\sigma_i^2}\right)\sum_{j'=0}^{\infty}\frac{1}{j'!}\left(\frac{s_i^2w_{z_{\mathrm{eq_i}}}^2}{8\sigma_i^4}\right)^{j'}\sum_{l=1}^{2+j'}\frac{\prod_{k=1,k\ne l}^{2+j'}\Gamma(\mathcal{F}_k-\mathcal{F}_l)\Gamma(\mathcal{F}_l)}{\prod_{k=2}^{2+j'}\Gamma(\mathcal{E}_k-\mathcal{F}_l)\Gamma(1+\mathcal{F}_l)}\left(\frac{1}{\lambda_iA_i}\sqrt{\hat{\gamma}_{\mathrm{th}}^{p,i}}\right)^{\mathcal{F}_l}\\ +\frac{(1-\omega_i)\rho_i^2\exp\left(\frac{-s_i^2}{2\sigma_i^2}\right)}{\Gamma(a_i)c_i}\sum_{j'=0}^{\infty}\frac{1}{j'!}\left(\frac{s_i^2w_{z_{\mathrm{eq_i}}}^2}{8\sigma_i^4}\right)^{j'}\sum_{l=1}^{2+j'}\frac{\prod_{k=1,k\ne l}^{2+j'}\Gamma(\mathcal{H}_k-\mathcal{H}_l)\Gamma(\mathcal{H}_l)}{\prod_{k=2}^{2+j'}\Gamma(\mathcal{G}_k-\mathcal{H}_l)\Gamma(1+\mathcal{H}_l)}\left(\frac{1}{b_iA_i}\sqrt{\hat{\gamma}_{\mathrm{th}}^{p,i}}\right)^{c_i\mathcal{H}_l}, & \text{if } \hat{\gamma}_{\mathrm{th}}^{c,i}\le\hat{\gamma}_{\mathrm{th}}^{p,i}\\ \omega_i\rho_i^2\exp\left(\frac{-s_i^2}{2\sigma_i^2}\right)\sum_{j'=0}^{\infty}\frac{1}{j'!}\left(\frac{s_i^2w_{z_{\mathrm{eq_i}}}^2}{8\sigma_i^4}\right)^{j'}\sum_{l=1}^{2+j'}\frac{\prod_{k=1,k\ne l}^{2+j'}\Gamma(\mathcal{F}_k-\mathcal{F}_l)\Gamma(\mathcal{F}_l)}{\prod_{k=2}^{2+j'}\Gamma(\mathcal{E}_k-\mathcal{F}_l)\Gamma(1+\mathcal{F}_l)}\left(\frac{1}{\lambda_iA_i}\sqrt{\hat{\gamma}_{\mathrm{th}}^{c,i}}\right)^{\mathcal{F}_l}\\ +\frac{(1-\omega_i)\rho_i^2\exp\left(\frac{-s_i^2}{2\sigma_i^2}\right)}{\Gamma(a_i)c_i}\sum_{j'=0}^{\infty}\frac{1}{j'!}\left(\frac{s_i^2w_{z_{\mathrm{eq_i}}}^2}{8\sigma_i^4}\right)^{j'}\sum_{l=1}^{2+j'}\frac{\prod_{k=1,k\ne l}^{2+j'}\Gamma(\mathcal{H}_k-\mathcal{H}_l)\Gamma(\mathcal{H}_l)}{\prod_{k=2}^{2+j'}\Gamma(\mathcal{G}_k-\mathcal{H}_l)\Gamma(1+\mathcal{H}_l)}\left(\frac{1}{b_iA_i}\sqrt{\hat{\gamma}_{\mathrm{th}}^{c,i}}\right)^{c_i\mathcal{H}_l}, & \text{if } \hat{\gamma}_{\mathrm{th}}^{c,i}\ge\hat{\gamma}_{\mathrm{th}}^{p,i}\end{cases} \tag{20}$$

be evaluated as follows:

$$\eta_i = \frac{(1 - P_{\mathrm{out_i}})R_i}{2}, \quad (21)$$

where $R_i = \min\{R_{c,i}, R_{p,i}\}$ with $R_{c,i}$ and $R_{p,i}$ representing the target rates for decoding the common and private messages, respectively.

The sum throughput of the overall system can be given as:

$$\eta_{\mathrm{sys}} = \sum_i^N \eta_i \quad (22)$$

B. SUM ERGODIC CAPACITY

For RSMA, the sum ergodic capacity of the system can be calculated by adding the minimum capacity of the common message among all users and the sum of the capacities of the private messages of all users. Therefore, the sum ergodic capacity can be expressed as follows [23]:

$$\xi_s = \min_{i\in\{1,2,\ldots,N\}} \xi_{c,i} + \sum_{i=1}^{N} \xi_{p,i}, \quad (23)$$

where $\xi_{c,i} = \int_0^\infty \log_2(1+\gamma_{c,i}) f_{\gamma_i}(\gamma)d\gamma$ and $\xi_{p,i} = \int_0^\infty \log_2(1+\gamma_{p,i}) f_{\gamma_i}(\gamma)d\gamma$.

In the following lemma, we derive the analytical expressions for the sum ergodic capacity.

Lemma 2: The analytical expression of the sum ergodic capacity of RSMA-based multi-user UOWC over EGG distributed oceanic turbulence and generalized PE is given in (24), at the bottom of the page, where $\xi_{c,a_1} = \{0, \{\frac{\rho_i^2+1}{2}\}^{j'+1}, \{\frac{\rho_i^2+2}{2}\}^{j'+1}\}$, $\xi_{c,b_1} = \{0, \frac{1}{2}, 1, \{\frac{\rho_i^2}{2}\}^{j'+1}, \{\frac{\rho_i^2+1}{2}\}^{j'+1}\}$, $\xi_{c,a_2} = \{0, \ldots, \frac{c_i-1}{c_i}, \{\frac{\rho_i^2+c_i}{2c_i}\}^{j'+1}, \{\frac{\rho_i^2+2c_i}{2c_i}\}^{j'+1}\}$, $\xi_{c,b_2} = \{0, \ldots, \frac{c_i-1}{c_i}, \frac{a_i}{2}, \frac{a_i+1}{2}, \{\frac{\rho_i^2}{2c_i}\}^{j'+1}, \{\frac{\rho_i^2+c_i}{2c_i}\}^{j'+1}\}$, $\mu_1 = \sum_{j'=0}^{j'+1}\{\rho_i^2\}^{j'+1} + \sum_{j'=0}^{j'+1}\{\rho_i^2+1\}^{j'+1} + \frac{3}{2}$, $\mu_2 = a_i + \sum_{j'=0}^{j'+1}\{\frac{\rho_i^2}{c_i}\}^{j'+1} + \sum_{j'=0}^{j'+1}\{\frac{\rho_i^2}{c_i}+1\}^{j'+1} + \frac{1}{2}$, $c^* = \frac{1}{2} + 2j'$, $\xi_{p,a_1} = \xi_{c,a_1}$, $\xi_{p,b_1} = \xi_{c,b_1}$, $\xi_{p,a_2} = \xi_{c,a_2}$, and $\xi_{p,b_2} = \xi_{c,b_2}$.

Proof: First, we evaluate the ergodic capacity for the common message using the following expression:

$$\xi_{c,i} = \int_0^\infty \log_2(1+\gamma_{c,i}) f_{\gamma_i}(\gamma)d\gamma, \quad (25)$$

Applying the approximation $\log(1+x) \approx \frac{2x}{(2+x)}$ [40] in (25), we get:

$$\xi_{c,i} \simeq \int_0^\infty \frac{2\gamma_{c,i}}{\ln(2)(2+\gamma_{c,i})} f_{\gamma_i}(\gamma)d\gamma. \quad (26)$$

To compute the above integral, we substitute (6) and (8) in (26), yielding:

$$\begin{aligned}\xi_{c,i} \simeq\; & \frac{a_c\omega_i\rho_i^2 \exp\left(\frac{-s_i^2}{2\sigma_i^2}\right)}{2\ln(2)} \sum_{j'=0}^{\infty}\frac{1}{j'!}\left(\frac{s_i^2 w_{z_{\mathrm{eq_i}}}^2}{8\sigma_i^4}\right)^{j'} \int_0^\infty \frac{\gamma^{1-1}}{(1+\gamma)} \\ & \times G_{1+j',2+j'}^{2+j',0}\left(\begin{matrix}\{\rho_i^2+1\}^{j'+1} \\ 1, \{\rho_i^2\}^{j'+1}\end{matrix}\middle| \frac{1}{\lambda_i A_i}\sqrt{\frac{\gamma}{\gamma_0}}\right)d\gamma \\ & + \frac{a_c(1-\omega_i)\rho_i^2 \exp\left(\frac{-s_i^2}{2\sigma_i^2}\right)}{2\ln(2)\Gamma(a_i)} \sum_{j'=0}^{\infty}\frac{1}{j'!}\left(\frac{s_i^2 w_{z_{\mathrm{eq_i}}}^2}{8\sigma_i^4}\right)^{j'} \int_0^\infty \frac{\gamma^{1-1}}{(1+\gamma)} \\ & \times G_{1+j',2+j'}^{2+j',0}\left(\begin{matrix}\{\frac{\rho_i^2}{c_i}+1\}^{j'+1} \\ a_i, \{\frac{\rho_i^2}{c_i}\}^{j'+1}\end{matrix}\middle| \left(\frac{1}{b_i A_i}\sqrt{\frac{\gamma}{\gamma_0}}\right)^{c_i}\right)d\gamma. \end{aligned} \quad (27)$$

Applying the identity [39, eq. (07).34.21.0086.01], we get the analytical expression of the ergodic capacity for the common message:

$$\xi_{c,i} \simeq \frac{2^{\mu_1-1}a_c\omega_i\rho_i^2 \exp\left(\frac{-s_i^2}{2\sigma_i^2}\right)}{(2\pi)^{c^*}\ln(2)} \sum_{j'=0}^{\infty}\frac{1}{j'!}\left(\frac{s_i^2 w_{z_{\mathrm{eq_i}}}^2}{8\sigma_i^4}\right)^{j'}$$

$$\begin{aligned}\xi_s \simeq\; & \min_{i\in\{1,2,\ldots,N\}}\left[\frac{2^{\mu_1-1}a_c\omega_i\rho_i^2 \exp\left(\frac{-s_i^2}{2\sigma_i^2}\right)}{(2\pi)^{c^*}\ln(2)} \sum_{j'=0}^{\infty}\frac{1}{j'!}\left(\frac{s_i^2 w_{z_{\mathrm{eq_i}}}^2}{8\sigma_i^4}\right)^{j'} G_{3+2j',5+2j'}^{5+2j',1}\left(\begin{matrix}\xi_{c,a_1} \\ \xi_{c,b_1}\end{matrix}\middle| \frac{1}{4\lambda_i^2 A_i^2\gamma_0}\right)\right. \\ & \left. + \frac{2^{\mu_2-1}a_c(1-\omega_i)\rho_i^2 \exp\left(\frac{-s_i^2}{2\sigma_i^2}\right)}{(2\pi)^{c^*+c_i-1}\ln(2)\Gamma(a_i)} \sum_{j'=0}^{\infty}\frac{1}{j'!}\left(\frac{s_i^2 w_{z_{\mathrm{eq_i}}}^2}{8\sigma_i^4}\right)^{j'} G_{2+2j'+c_i,4+2j'+c_i}^{4+2j'+c_i,c_i}\left(\begin{matrix}\xi_{c,a_2} \\ \xi_{c,b_2}\end{matrix}\middle| \frac{1}{4(b_iA_i\sqrt{\gamma_0})^{2c_i}}\right)\right] \\ & + \sum_{i=1}^{N}\left[\frac{2^{\mu_1-1}a_{p_i}\omega_i\rho_i^2 \exp\left(\frac{-s_i^2}{2\sigma_i^2}\right)}{(2\pi)^{c^*}(a_{p_i}+B)\ln(2)} \sum_{j'=0}^{\infty}\frac{1}{j'!}\left(\frac{s_i^2 w_{z_{\mathrm{eq_i}}}^2}{8\sigma_i^4}\right)^{j'} G_{3+2j',5+2j'}^{5+2j',1}\left(\begin{matrix}\xi_{p,a_1} \\ \xi_{p,b_1}\end{matrix}\middle| \frac{1}{4\lambda_i^2 A_i^2\gamma_0(a_{p_i}+B)}\right)\right. \\ & \left. + \frac{2^{\mu_2-1}a_{p_i}(1-\omega_i)\rho_i^2 \exp\left(\frac{-s_i^2}{2\sigma_i^2}\right)}{(2\pi)^{c^*+c_i-1}\ln(2)\Gamma(a_i)(a_{p_i}+B)} \sum_{j'=0}^{\infty}\frac{1}{j'!}\left(\frac{s_i^2 w_{z_{\mathrm{eq_i}}}^2}{8\sigma_i^4}\right)^{j'} G_{2+2j'+c_i,4+2j'+c_i}^{4+2j'+c_i,c_i}\left(\begin{matrix}\xi_{p,a_2} \\ \xi_{p,b_2}\end{matrix}\middle| \frac{1}{4(b_iA_i\sqrt{\gamma_0})^{2c_i}(a_{p_i}+B)^{c_i}}\right)\right] \end{aligned} \quad (24)$$

$$\times G_{3+2j',5+2j'}^{5+2j',1}\left(\begin{matrix}\xi_{c,a_1}\\ \xi_{c,b_1}\end{matrix}\middle|\frac{1}{4\lambda_i^2A_i^2\gamma_0}\right)$$
$$+\frac{2^{\mu_2-1}a_c(1-\omega_i)\rho_i^2\exp\left(\frac{-s_i^2}{2\sigma_i^2}\right)}{(2\pi)^{c^*+c_i-1}\ln(2)\Gamma(a_i)}\sum_{j'=0}^{\infty}\frac{1}{j'!}\left(\frac{s_i^2w_{z_{\mathrm{eq_i}}}^2}{8\sigma_i^4}\right)^{j'}$$
$$\times G_{2+2j'+c_i,4+2j'+c_i}^{4+2j'+c_i,c_i}\left(\begin{matrix}\xi_{c,a_2}\\ \xi_{c,b_2}\end{matrix}\middle|\frac{1}{4\left(b_iA_i\sqrt{\gamma_0}\right)^{2c_i}}\right). \tag{28}$$

Similarly, we determine the ergodic capacity for the private message using the following expression:

$$\xi_{p,i}\simeq\int_0^{\infty}\frac{2\gamma_{p,i}}{\ln(2)\left(2+\gamma_{p,i}\right)}f_{\gamma_i}(\gamma)d\gamma. \tag{29}$$

To solve the above integral, we substitute (7) and (8) into (29) as follows:

$$\xi_{p,i}\simeq\frac{a_{p_i}\omega_i\rho_i^2\exp\left(\frac{-s_i^2}{2\sigma_i^2}\right)}{2\ln(2)\left(a_{p_i}+B\right)}\sum_{j'=0}^{\infty}\frac{1}{j'!}\left(\frac{s_i^2w_{z_{\mathrm{eq_i}}}^2}{8\sigma_i^4}\right)^{j'}\int_0^{\infty}\frac{\gamma^{1-1}}{(B+\gamma)}$$
$$\times G_{1+j',2+j'}^{2+j',0}\left(\begin{matrix}\{\rho_i^2+1\}^{j'+1}\\ 1,\{\rho_i^2\}^{j'+1}\end{matrix}\middle|\frac{1}{\lambda_iA_i}\sqrt{\frac{\gamma}{\gamma_0}}\right)d\gamma$$
$$+\frac{a_{p_i}(1-\omega_i)\rho_i^2\exp\left(\frac{-s_i^2}{2\sigma_i^2}\right)}{2\ln(2)\left(a_{p_i}+B\right)\Gamma(a_i)}$$
$$\times\sum_{j'=0}^{\infty}\frac{1}{j'!}\left(\frac{s_i^2w_{z_{\mathrm{eq_i}}}^2}{8\sigma_i^4}\right)^{j'}\int_0^{\infty}\frac{\gamma^{1-1}}{(B+\gamma)}$$
$$\times G_{1+j',2+j'}^{2+j',0}\left(\begin{matrix}\{\frac{\rho_i^2}{c_i}+1\}^{j'+1}\\ a_i,\{\frac{\rho_i^2}{c_i}\}^{j'+1}\end{matrix}\middle|\left(\frac{1}{b_iA_i}\sqrt{\frac{\gamma}{\gamma_0}}\right)^{c_i}\right)d\gamma. \tag{30}$$

Applying the identity [39, eq. (07).34.21.0086.01], we get an approximation of the ergodic capacity for the private message:

$$\xi_{p,i}\simeq\frac{2^{\mu_1-1}a_{p_i}\omega_i\rho_i^2\exp\left(\frac{-s_i^2}{2\sigma_i^2}\right)}{(2\pi)^{c^*}\left(a_{p_i}+B\right)\ln(2)}\sum_{j'=0}^{\infty}\frac{1}{j'!}\left(\frac{s_i^2w_{z_{\mathrm{eq_i}}}^2}{8\sigma_i^4}\right)^{j'}$$
$$\times G_{3+2j',5+2j'}^{5+2j',1}\left(\begin{matrix}\xi_{p,a_1}\\ \xi_{p,b_1}\end{matrix}\middle|\frac{1}{4\lambda_i^2A_i^2\gamma_0\left(a_{p_i}+B\right)}\right)$$
$$+\frac{2^{\mu_2-1}a_{p_i}(1-\omega_i)\rho_i^2\exp\left(\frac{-s_i^2}{2\sigma_i^2}\right)}{(2\pi)^{c^*+c_i-1}\ln(2)\Gamma(a_i)\left(a_{p_i}+B\right)}\sum_{j'=0}^{\infty}\frac{1}{j'!}\left(\frac{s_i^2w_{z_{\mathrm{eq_i}}}^2}{8\sigma_i^4}\right)^{j'}$$
$$\times G_{2+2j'+c_i,4+2j'+c_i}^{4+2j'+c_i,c_i}\left(\begin{matrix}\xi_{p,a_2}\\ \xi_{p,b_2}\end{matrix}\middle|\frac{1}{4\left(b_iA_i\sqrt{\gamma_0}\right)^{2c_i}\left(a_{p_i}+B\right)^{c_i}}\right). \tag{31}$$

Therefore, the sum ergodic capacity in (24) is obtained by substituting (28) and (31) in (23). ■

Finally, we derive an asymptotic expression for the sum ergodic capacity of RSMA-based UOWC over EGG-distributed oceanic turbulence and generalized PE in the following Lemma.

Lemma 3: The asymptotic sum ergodic capacity of RSMA-based UOWC at high SNR ($\gamma_0\to\infty$) is given in (32), at the bottom of the page, where $\mathcal{A}_k=\mathcal{A}_l=\{0,\{\frac{\rho_i^2+1}{2}\}^{j'+1},\{\frac{\rho_i^2+2}{2}\}^{j'+1}\}$, $\mathcal{B}_k=\mathcal{B}_l=\{0,\frac{1}{2},1,\{\frac{\rho_i^2}{2}\}^{j'+1},\{\frac{\rho_i^2+1}{2}\}^{j'+1}\}$, $\mathcal{C}_k=\mathcal{C}_l=\{0,\ldots,\frac{c_i-1}{c_i},\{\frac{\rho_i^2+c_i}{2c_i}\}^{j'+1},\{\frac{\rho_i^2+2c_i}{2c_i}\}^{j'+1}\}$ and, $\mathcal{D}_k=\mathcal{D}_l=\{0,\ldots,\frac{c_i-1}{c_i},\frac{a_i}{2},\frac{a_i+1}{2},\{\frac{\rho_i^2}{2c_i}\}^{j'+1},\{\frac{\rho_i^2+c_i}{2c_i}\}^{j'+1}\}$.

$$\xi_s^{\infty}=\min_{i\in\{1,2,\ldots,N\}}\left[\frac{2^{\mu_1-1}a_c\omega_i\rho_i^2\exp\left(\frac{-s_i^2}{2\sigma_i^2}\right)}{(2\pi)^{c^*}\ln(2)}\sum_{j'=0}^{\infty}\frac{1}{j'!}\left(\frac{s_i^2w_{z_{\mathrm{eq_i}}}^2}{8\sigma_i^4}\right)^{j'}\sum_{l=1}^{5+2j'}\frac{\Gamma(1+\mathcal{B}_l)\prod_{k=1,k\neq l}^{5+2j'}\Gamma(\mathcal{B}_k-\mathcal{B}_l)}{\prod_{k=2}^{3+2j'}\Gamma(\mathcal{A}_k-\mathcal{B}_l)}\left(\frac{1}{4\lambda_i^2A_i^2\gamma_0}\right)^{\mathcal{B}_l}\right.$$
$$+\frac{2^{\mu_2-1}a_c(1-\omega_i)\rho_i^2\exp\left(\frac{-s_i^2}{2\sigma_i^2}\right)}{(2\pi)^{c^*+c_i-1}\ln(2)\Gamma(a_i)}\sum_{j'=0}^{\infty}\frac{1}{j'!}\left(\frac{s_i^2w_{z_{\mathrm{eq_i}}}^2}{8\sigma_i^4}\right)^{j'}\sum_{l=1}^{4+2j'+c_i}\frac{\prod_{k=1,k\neq l}^{4+2j'+c_i}\Gamma(\mathcal{D}_k-\mathcal{D}_l)\prod_{k=1}^{c_i}\Gamma(1-\mathcal{C}_k+\mathcal{D}_l)}{\prod_{k=c_i+1}^{2+2j'+c_i}\Gamma(\mathcal{C}_k-\mathcal{D}_l)}$$
$$\left.\times\left(\frac{1}{4\left(b_iA_i\sqrt{\gamma_0}\right)^{2c_i}}\right)^{\mathcal{D}_l}\right]+\sum_{i=1}^{N}\left[\frac{2^{\mu_1-1}a_{p_i}\omega_i\rho_i^2\exp\left(\frac{-s_i^2}{2\sigma_i^2}\right)}{(2\pi)^{c^*}\left(a_{p_i}+B\right)\ln(2)}\sum_{j'=0}^{\infty}\frac{1}{j'!}\left(\frac{s_i^2w_{z_{\mathrm{eq_i}}}^2}{8\sigma_i^4}\right)^{j'}\sum_{l=1}^{5+2j'}\frac{\Gamma(1+\mathcal{B}_l)\prod_{k=1,k\neq l}^{5+2j'}\Gamma(\mathcal{B}_k-\mathcal{B}_l)}{\prod_{k=2}^{3+2j'}\Gamma(\mathcal{A}_k-\mathcal{B}_l)}\right.$$
$$\times\left(\frac{1}{4\lambda_i^2A_i^2\gamma_0\left(a_{p_i}+B\right)}\right)^{\mathcal{B}_l}+\frac{2^{\mu_2-1}a_{p_i}(1-\omega_i)\rho_i^2\exp\left(\frac{-s_i^2}{2\sigma_i^2}\right)}{(2\pi)^{c^*+c_i-1}\ln(2)\Gamma(a_i)\left(a_{p_i}+B\right)}\sum_{j'=0}^{\infty}\frac{1}{j'!}\left(\frac{s_i^2w_{z_{\mathrm{eq_i}}}^2}{8\sigma_i^4}\right)^{j'}$$
$$\left.\times\sum_{l=1}^{4+2j'+c_i}\frac{\prod_{k=1,k\neq l}^{4+2j'+c_i}\Gamma(\mathcal{D}_k-\mathcal{D}_l)\prod_{k=1}^{c_i}\Gamma(1-\mathcal{C}_k+\mathcal{D}_l)}{\prod_{k=c_i+1}^{2+2j'+c_i}\Gamma(\mathcal{C}_k-\mathcal{D}_l)}\left(\frac{1}{4\left(b_iA_i\sqrt{\gamma_0}\right)^{2c_i}\left(a_{p_i}+B\right)^{c_i}}\right)^{\mathcal{D}_l}\right] \tag{32}$$

Proof: Taking the asymptotic expansion of the Meijer-G function, [39, eq. (07).34.06.0006.01] at high SNR $\gamma_0 \to \infty$ in (24), we get (32). ■

Remark 3: We can further determine the diversity order of the proposed system as $G_i = \min\{\frac{1}{2}, \frac{\rho_i^2}{2}, \frac{a_i c_i}{2}\}$ by evaluating the exponent of γ_0 in the asymptotic expression of the sum ergodic capacity in (32). It is important to highlight that both MATLAB and MATHEMATICA provide standard computational built-in functions for calculating Meijer-G functions [39]. Additionally, the PDF of the SNR over oceanic turbulence and generalized PE enables precise statistical analysis and an accurate asymptotic representation using Gamma functions. This allows for a comprehensive evaluation of RSMA-based multi-user UOWC systems' performance and an understanding of the impact of various parameters on the system performance. In contrast, numerical integration may not provide straightforward insights into the system's performance. It is worth mentioning that Monte Carlo simulations, although feasible, require longer computational time to assess the performance of the considered system.

V. SIMULATION RESULTS AND DISCUSSIONS

In this section, we assess the performance of the proposed downlink RSMA-based multi-user UOWC system under EGG turbulence with zero boresight PE. We consider a distance $d = 50$m between the source and the users. Two different bubble levels (BLs) are considered to evaluate the system performance, namely BL= 2.4 and BL=16.5. Two different PE parameters are considered for simulations, namely ($A_i = 0.04$, $\rho^2 = 3.5377$) and ($A_i = 0.054$, $\rho^2 = 37.0657$). The SNR threshold is set to $\gamma_{th} = 6$ dB. Utilizing Monte-Carlo (MC) simulation averaged across 10^7 channel realizations, we validate the derived analytical expressions. Moreover, the asymptotic expression of the outage probability aligns with both the analytical and simulation results in the high SNR range. For the computation of the Meijer-G function, we utilize the standard built-in MATLAB library "meijerG". The simulation parameters are summarized in Table 2. We consider the outage probability, the throughput, and the sum ergodic capacity metrics in evaluating the performance of the proposed system.

A. OUTAGE PROBABILITY

First, we analyze the outage probability performance of the proposed system as a function of the PE parameters and resource distribution between common and private channels. Fig. 2 depicts the effect of the change in turbulence and PE parameters on the outage probability of the second user P_{out_2}. We can observe that the simulation and derived analytical results provide the same results. It is also noticed that $BL = 2.4$ yields 88% less outage probability at 25 dBm than $BL = 16.5$, and the PE parameters ($A_i = 0.054$, $\rho^2 = 37.0657$) yield 23% less outage probability at 25 dBm than ($A_i = 0.04$, $\rho^2 = 3.5377$). This is because increasing these variables decreases the PE effect, which decreases the outage probability of the system. Fig. 3 analyzes the second user's outage probability performance for different values of the parameter a_c while keeping an equal distribution among a_{p_i}s. It is observed that increasing a_c from 0.5 to 0.6 decreases the

TABLE 2. Simulation parameters.

Parameters	Notations	Values	Unit
Transmitted power	P_t	0 to 25	dBm
Distance	d	50	m
Threshold SNR	γ_{th}	6	dB
Extinction coefficient	α	0.056	-
Turbulence parameters	$\{\omega, \lambda, a, b, c\}$	BL(2.4)={0.1770,0.4687, 0.7736,1.1372,49.1773} BL(16.5) = {0.5117, 0.1602, 0.0075,2.9963,216.8356}	-
PE	$\{A_i, \rho^2\}$	{0.04,3.5377} {0.054,37.0657}	-
Normalized beam-width	w_{z_i}/r_i	{5,8}	-
Jitter standard deviation	σ_i	{8,24}	-
Horizontal displacement	μ_{x_i}	0.1	m
Vertical displacement	μ_{y_i}	0.1	m

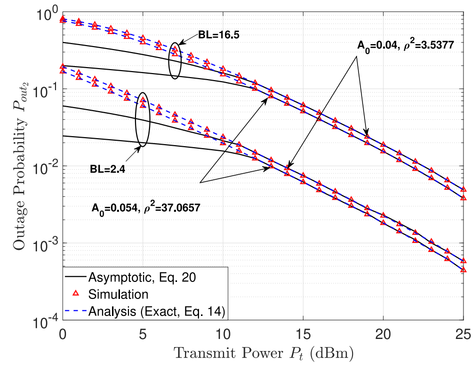

FIGURE 2. Outage probability performance of RSMA-based multi-user UOWC for $N = 5$, $a_c = 0.5$, and $a_{p_i} = 0.1, i = \{1\ldots N\}$.

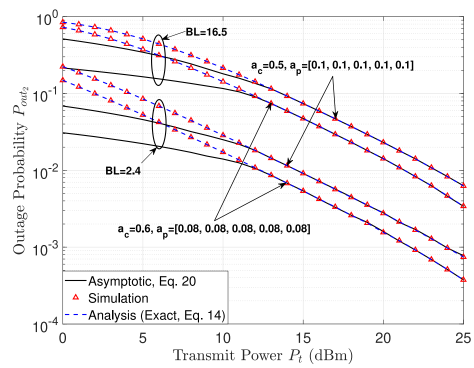

FIGURE 3. Outage probability performance of RSMA-based multi-user UOWC for $N = 5$ and PE parameters $A_i = 0.04$ and $\rho^2 = 3.5377$.

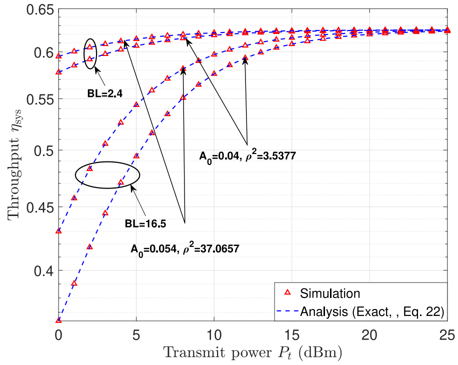

FIGURE 4. **Throughput performance of RSMA-based multi-user UOWC for $N = 5$, $a_c = 0.5$, $a_{p_i} = 0.1$, $i = 1\ldots N$, and PE parameters $A_i = 0.04$ and $\rho^2 = 3.5377$ and $A_i = 0.054$ and $\rho^2 = 37.0657$.**

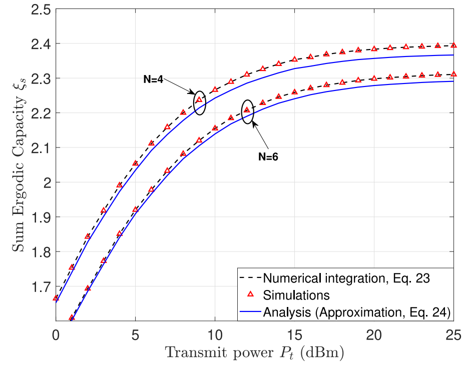

FIGURE 6. **Sum ergodic capacity performance of RSMA-based multi-user UOWC for $BL = 16.5$, $a_c = \{0.4, 0.4\}$, and $a_{p_i} = \{0.15, 0.1\}$, $i = 1\ldots N$, and PE parameters $A_i = 0.04$ and $\rho^2 = 3.5377$.**

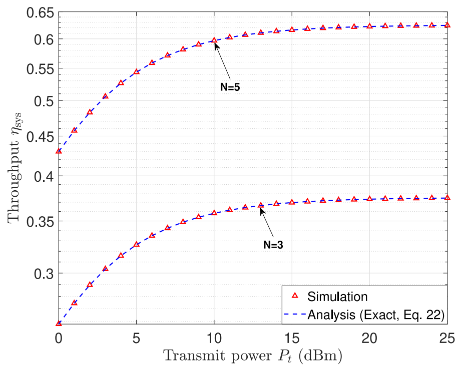

FIGURE 5. **Throughput performance of RSMA-based multi-user UOWC for $BL = 16.5$, $a_c = \{0.5, 0.5\}$, $a_{p_i} = \{0.1, 1/6\}$, $i = 1\ldots N$, and PE parameters $A_i = 0.054$ and $\rho^2 = 37.0657$.**

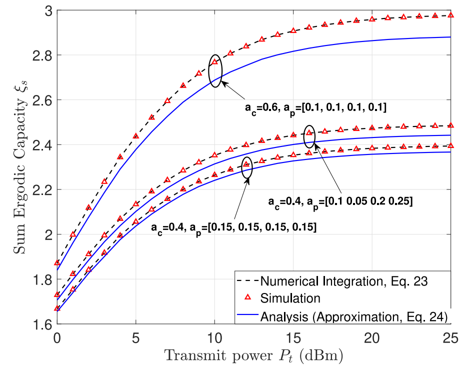

FIGURE 7. **Sum ergodic capacity performance of RSMA-based multi-user UOWC for $BL = 16.5$ and $N = 4$, and PE parameters $A_i = 0.04$ and $\rho^2 = 3.5377$.**

outage by 45% at 25 dBm. Hence, it can be deduced that the common channel power allocation significantly affects the system performance. Furthermore, the slope of the outage probability aligns with the diversity order of the system $G_i = \min\{\frac{1}{2}, \frac{\rho_i^2}{2}, \frac{a_i c_i}{2}\}$.

B. THROUGHPUT

Second, we evaluate the throughput performance of the proposed RSMA-based multi-user UOWC system. We set $R_{c,1} = R_{c,2} = R_{c,3} = R_{c,4} = R_{c,5} = 1$ and $R_{p,1} = 0.5$, $R_{p,2} = 0.25$, $R_{p,3} = 0.45$, $R_{p,4} = 0.35$, $R_{p,5} = 0.4$. Fig. 4 demonstrates the performance of the system's throughput η_{sys} for different oceanic turbulence and PE parameters. The throughput is an increasing function of the transmit power since increasing power improves the link quality. Also, $BL = 2.4$ yields 23% higher throughput than $BL = 16.5$ at 5 dBm, while decreasing the PE parameters from ($A_i = 0.054$, $\rho^2 = 37.0657$) to ($A_i = 0.04$, $\rho^2 = 3.5377$) decreases the throughput by 9% at 5 dBm. This aligns with the results found in Fig. 2 for outage probability. At high transmit power P_t, the performance of the system is similar for different oceanic turbulence and PE parameters. Fig. 5 shows the effect of the number of users on the system throughput η_{sys}. In fact, increasing the number of users from three to five increases the throughput by 67% at 5 dBm. This can be explained by the fact that having more users will allow more efficient spectrum use since the available bandwidth is shared by more users.

C. SUM ERGODIC CAPACITY

Finally, we assess the sum ergodic capacity performance of the considered system for $BL = 16.5$ and PE parameters $A_i = 0.04$ and $\rho^2 = 3.5377$. We evaluate the effect of the number of users and the power distribution between the common channel a_c and private channels a_ps. Fig. 6 shows the sum ergodic capacity as a function of the transmit power for 4 and 6 users. The sum ergodic capacity is an increasing function of the transmit power, which aligns with the theory that increasing the power improves the link quality. The results also show that the simulations match the numerical results, which validates the accuracy of our analysis. Furthermore, the sum ergodic capacity decreases when increasing the number of users from four to six by 3.6% at 25 dBm transmit power, which can be explained by the fact that adding more users to the system increases interference. Fig. 7 presents the sum ergodic capacity as a function of the transmit power for four users. We consider two different values for a_c while equally dividing the remaining power among the private channels. Moreover, we evaluate the performance of the proposed system by maintaining a fixed value for $a_c = 0.4$ and dividing the rest of the power resource equally or unequally between the private links. We observe that changing the value of a_c from 0.4 to 0.6 increased the sum ergodic capacity by 24% at 25 dBm while moving from an equal to unequal distribution of a_p increases the sum ergodic capacity by only 3.6% at 25 dBm. Hence, we can say that common channel power allocation has a stronger effect on the system performance than private channel power allocation.

Finally, we can conclude that decreasing the effect of PE by increasing the values of its parameters enhances the performance of the system. Also, increasing the BL decreases the performance of the system as it strengthens the oceanic turbulence. Moreover, the common channel power allocation significantly controls the performance of the system.

VI. CONCLUSION

The presence of oceanic turbulence and PE poses significant challenges to UOWC systems, affecting their performance and reliability. To overcome these challenges, RSMA has been employed as a promising multiple-access technique that optimizes resource allocation in the presence of interference. Through statistical characterization, outage probability analysis, and evaluation of throughput and sum ergodic capacity, we have gained valuable insights into the performance of RSMA-based UOWC systems in oceanic turbulence channels with PE. Our results demonstrate that by appropriately allocating the power coefficients and setting the target rates, RSMA allows for efficient transmission and reception of both common and private messages, enhancing the overall system performance.

The analytical expressions and asymptotic analysis presented in this study provide valuable guidance for the design and optimization of RSMA-based UOWC systems. By carefully selecting parameters and considering the system constraints, such as transmit power, power coefficients, and target rates, the performance of UOWC systems can be significantly improved. Overall, the findings of this study emphasize the importance of RSMA in addressing the challenges posed by oceanic turbulence and PE in UOWC systems. Further research can focus on exploring advanced techniques and algorithms to enhance the performance and reliability of UOWC systems, ultimately enabling robust UOWCs in challenging underwater environments.

REFERENCES

[1] Z. Zeng, S. Fu, H. Zhang, Y. Dong, and J. Cheng, "A survey of underwater optical wireless communications," *IEEE Commun. Surveys Tuts.*, vol. 19, no. 1, pp. 204–238, 1st Quart., 2017.

[2] H. Kulhandjian, "Inside out: Underwater communications," *J. Ocean Technol.*, vol. 9, no. 2, pp. 104–105, 2014.

[3] S. Jiang, "On reliable data transfer in underwater acoustic networks: A survey from networking perspective," *IEEE Commun. Surveys Tuts.*, vol. 20, no. 2, pp. 1036–1055, 2nd Quart., 2018.

[4] M. Erol-Kantarci, H. T. Mouftah, and S. Oktug, "A survey of architectures and localization techniques for underwater acoustic sensor networks," *IEEE Commun. Surveys Tuts.*, vol. 13, no. 3, pp. 487–502, 3rd Quart., 2011.

[5] A. Celik, I. Romdhane, G. Kaddoum, and A. M. Eltawil, "A top-down survey on optical wireless communications for the Internet of Things," *IEEE Commun. Surveys Tuts.*, vol. 25, no. 1, pp. 1–45, 1st Quart., 2023.

[6] Y. Jiang, Y. Li, X. Zhang, M. Ju, and P. Huang, "Outage performance analysis for relay-assisted UWOC systems over GGD weak turbulence with nonzero boresight pointing errors," *Physical Commun.*, vol. 58, Jun. 2023, Art. no. 102017.

[7] W. Jiang, W. Liu, and Z. Xu, "Experimental investigation of turbulence channel characteristics for underwater optical wireless communications," in *Proc. IEEE/CIC Int. Conf. Commun. China (ICCC)*, 2021, pp. 858–863.

[8] E. Zedini, H. M. Oubei, A. Kammoun, M. Hamdi, B. S. Ooi, and M.-S. Alouini, "Unified statistical channel model for turbulence-induced fading in underwater wireless optical communication systems," *IEEE Trans. Commun.*, vol. 67, no. 4, pp. 2893–2907, Apr. 2019.

[9] Y. Mao, B. Clerckx, and V. O. K. Li, "Rate-splitting multiple access for downlink communication systems: Bridging, generalizing, and outperforming SDMA and NOMA," *EURASIP J. Wireless Commun. Netw.*, vol. 2018, pp. 1–54, May 2018.

[10] M. Elsayed, A. Samir, A. A. El-Banna, W. U. Khan, S. Chatzinotas, and B. M. ElHalawany, "Mixed RIS-relay NOMA-based RF-UOWC systems," in *Proc. IEEE 95th Veh. Technol. Conf. (VTC2022)*, 2022, pp. 1–6.

[11] M. Le-Tran and S. Kim, "Performance analysis of multi-hop underwater wireless optical communication systems over exponential-generalized gamma turbulence channels," *IEEE Trans. Veh. Technol.*, vol. 71, no. 6, pp. 6214–6227, Jun. 2022.

[12] Y. Lou, J. Cheng, D. Nie, and G. Qiao, "Performance of vertical underwater wireless optical communications with cascaded layered modeling," *IEEE Trans. Veh. Technol.*, vol. 71, no. 5, pp. 5651–5655, May 2022.

[13] Z. Rahman, N. V. Tailor, S. M. Zafaruddin, and V. K. Chaubey, "Unified performance assessment of optical wireless communication over multi-layer underwater channels," *IEEE Photon. J.*, vol. 14, no. 5, pp. 1–14, Oct. 2022.

[14] Z. Rahman, S. M. Zafaruddin, and V. K. Chaubey, "Direct air-to-underwater optical wireless communication: Statistical characterization and outage performance," *IEEE Trans. Veh. Technol.*, vol. 72, no. 2, pp. 2655–2660, Feb. 2023.

[15] J. Sipani, D. Roy, and S. Anees, "On the performance of hybrid RF/UWOC system," in *Proc. 4th Int. Conf. Adv. Commun. Technol. Netw. (CommNet)*, 2021, pp. 1–5.

[16] A. S. M. Badrudduza et al., "Security at the physical layer over GG fading and mEGG turbulence induced RF-UOWC mixed system," *IEEE Access*, vol. 9, pp. 18123–18136, 2021.

[17] S. Yadav, A. Vats, M. Aggarwal, and S. Ahuja, "Performance analysis and altitude optimization of UAV-enabled dual-hop mixed RF-UWOC system," *IEEE Trans. Veh. Technol.*, vol. 70, no. 12, pp. 12651–12661, Dec. 2021.

[18] S. Li, L. Yang, D. B. Da Costa, and S. Yu, "Performance analysis of UAV-based mixed RF-UWOC transmission systems," *IEEE Trans. Commun.*, vol. 69, no. 8, pp. 5559–5572, Aug. 2021.

[19] S. Li, L. Yang, D. B. Da Costa, J. Zhang, and M.-S. Alouini, "Performance analysis of mixed RF-UWOC dual-hop transmission systems," *IEEE Trans. Veh. Technol.*, vol. 69, no. 11, pp. 14043–14048, Nov. 2020.

[20] L. Yang, Q. Zhu, S. Li, I. S. Ansari, and S. Yu, "On the performance of mixed FSO-UWOC dual-hop transmission systems," *IEEE Wireless Commun. Lett.*, vol. 10, no. 9, pp. 2041–2045, Sep. 2021.

[21] W. Jaafar, S. Naser, S. Muhaidat, P. C. Sofotasios, and H. Yanikomeroglu, "On the downlink performance of RSMA-based UAV communications," *IEEE Trans. Veh. Technol.*, vol. 69, no. 12, pp. 16258–16263, Dec. 2020.

[22] S. K. Singh, K. Agrawal, K. Singh, and C.-P. Li, "Outage probability and throughput analysis of UAV-assisted rate-splitting multiple access," *IEEE Wireless Commun. Lett.*, vol. 10, no. 11, pp. 2528–2532, Nov. 2021.

[23] S. K. Singh, K. Agrawal, K. Singh, and C.-P. Li, "Ergodic capacity and placement optimization for RSMA-enabled UAV-assisted communication," *IEEE Syst. J.*, vol. 17, no. 2, pp. 2586–2589, Jun. 2023.

[24] A. Bansal, N. Agrawal, and K. Singh, "Rate-splitting multiple access for UAV-based RIS-enabled interference-limited vehicular communication system," *IEEE Trans. Intell. Veh.*, vol. 8, no. 1, pp. 936–948, Jan. 2023.
[25] E. J. D. Santos, R. D. Souza, and J. L. Rebelatto, "Rate-splitting multiple access for URLLC uplink in physical layer network slicing with eMBB," *IEEE Access*, vol. 9, pp. 163178–163187, 2021.
[26] Z. Yang, J. Shi, Z. Li, M. Chen, W. Xu, and M. Shikh-Bahaei, "Energy efficient rate splitting multiple access (RSMA) with reconfigurable intelligent surface," in *Proc. IEEE Int. Conf. Commun. Workshops (ICC Workshops)*, 2020, pp. 1–6.
[27] W. U. Khan et al., "Rate splitting multiple access for next generation cognitive radio enabled LEO satellite networks," *IEEE Trans. Wireless Commun.*, vol. 22, no. 11, pp. 8423–8435, Nov. 2023
[28] S. Naser et al., "Rate-splitting multiple access: Unifying NOMA and SDMA in MISO VLC channels," *IEEE Open J. Veh. Technol.*, vol. 1, pp. 393–413, Oct. 2020.
[29] S. Ma et al., "Robust beamforming design for rate splitting multiple access-aided MISO visible light communications," 2021, *arXiv:2108.07014*.
[30] S. Ma, G. Zhang, Z. Zhang, R. Gu, Y. Wu, and S. Li, "Rate splitting multiple access-aided MISO visible light communications," in *Proc. Int. Symp. Wireless Commun. Syst. (ISWCS)*, 2022, pp. 1–6.
[31] F. Xing, S. He, V. C. M. Leung, and H. Yin, "Energy efficiency optimization for rate-splitting multiple access-based indoor visible light communication networks," *IEEE J. Sel. Areas Commun.*, vol. 40, no. 5, pp. 1706–1720, May 2022.
[32] S. Tao, H. Yu, Q. Li, Y. Tang, and D. Zhang, "One-layer rate-splitting multiple access with benefits over power-domain NOMA in indoor multi-cell visible light communication networks," in *Proc. IEEE Int. Conf. Commun. Workshops (ICC Workshops)*, 2020, pp. 1–7.
[33] F. Xing, S. He, Y. Yue, and H. Yin, "Ergodic rate characterization for rate-splitting multiple access based underwater wireless optical communications," in *Proc. IEEE 95th Veh. Technol. Conf. (VTC2022)*, 2022, pp. 1–7.
[34] D. Zwillinger, *Table of Integrals, Series, and Products*. Amsterdam, The Netherlands: Elsevier, 2014.
[35] L. Yang, X. Gao, and M.-S. Alouini, "Performance analysis of relay-assisted all-optical FSO networks over strong atmospheric turbulence channels with pointing errors," *J. Lightw. Technol.*, vol. 32, no. 23, pp. 4613–4620, Dec. 1, 2014.
[36] K.-J. Jung, S. S. Nam, M.-S. Alouini, and Y.-C. Ko, "Unified finite series approximation of FSO performance over strong turbulence combined with various pointing error conditions," *IEEE Trans. Commun.*, vol. 68, no. 10, pp. 6413–6425, Oct. 2020.
[37] A. A. Farid and S. Hranilovic, "Outage capacity optimization for free-space optical links with pointing errors," *J. Lightw. Technol.*, vol. 25, no. 7, pp. 1702–1710, Jul. 2007.
[38] Z. Rahman, S. M. Zafaruddin, and V. K. Chaubey, "Multihop optical wireless communication over $\mathcal{F}$-turbulence channels and generalized pointing errors with fog-induced fading," *IEEE Photon. J.*, vol. 14, no. 5, pp. 1–14, Oct. 2022.
[39] Wolfram function. "Functions/MeijerG." wolfram.com. Accessed: Jun. 12, 2021. [Online]. Available: https://functions.wolfram.com/hypergeometric
[40] F. Topsøe, "Some bounds for the logarithmic function," *RGMIA Res. Rep. Collect.*, vol. 7, no. 2, pp. 1–20, 2004.

ZIYAUR RAHMAN (Student Member, IEEE) received the B.Tech. and M.Tech. degrees in electronics and communication engineering from Punjab Technical University, Kapurthala, India, in 2015 and 2017, respectively, and the Ph.D. degree in wireless communications from the Birla Institute of Technology and Science (Pilani), Pilani, India, in 2023. He is currently working as a Postdoctoral Research Fellow in the area of underwater optical wireless communications with the Department of Electrical Engineering, École de Technologie Supérieure, University of Quebec, Montreal, Canada. His research interests include optical wireless communications for terrestrial and underwater applications and machine learning for communication systems.

IMENE ROMDHANE (Student Member) received the B.S. degree in telecommunication engineering from the École Supérieure de Communications de Tunis, Aryanah, Tunisia, in 2016, and the M.S. degree in electrical and electronics engineering from Bogazici University, Istanbul, Turkey, in 2019. She is currently pursuing the Ph.D. degree in electrical engineering with the École de Technologie Supérieure, Université du Québec, Montreal, QC, Canada. During her studies, she has focused on optical communications, including fiber communications, wireless optical communications, and underwater optical wireless communications. Also, she has shown interest in artificial intelligent by applying machine learning techniques, including reinforcement learning to the optical field.

GEORGES KADDOUM (Senior Member, IEEE) received the bachelor's degree in electrical engineering from the École nationale Supérieure de Techniques Avancés, France, the M.Sc. degree in telecommunications and signal processing from Telecom Bretagne, Brest, in 2005, and the Ph.D. degree in signal processing and telecommunications from the National Institute of Applied Sciences, Toulouse, France, in 2009. He is currently an Associate Professor and the Tier 2 Canada Research Chair with the École de Technologie Supérieure (ÉTS), University of Quebec, Montreal, Canada, and also a Faculty Fellow with the Cyber Security Systems and Applied AI Research Center, Lebanese American University, Beirut, Lebanon. He has published more than 300 journals and conference papers, two book chapters, and eight pending patents. His recent research activities cover wireless communication networks, resource allocations, security and space communications, and navigation. He received the Best Paper Award at the 2023 IEEE International Wireless Communications and Mobile Computing Conference, the 2017 IEEE International Symposium on Personal Indoor and Mobile Radio Communications, and the 2014 IEEE International Conference on Wireless and Mobile Computing, Networking, Communications. Moreover, he received the IEEE TRANSACTIONS ON COMMUNICATIONS Exemplary Reviewer Award in 2015, 2017, and 2019. In addition, he received the Research Excellence Award of the Université du Quebec in 2018. In 2019, he received the Research Excellence Award from ÉTS in recognition of his outstanding research outcomes. Finally, he received the IEEE TCSC Award for Excellence in Scalable Computing in 2022. He is currently serving as an Area Editor for the IEEE TRANSACTIONS ON MACHINE LEARNING IN COMMUNICATIONS AND NETWORKING and an Editor for IEEE TRANSACTIONS ON COMMUNICATIONS.